Packaging-ejection phase transitions of a polymer chain: Theory and Monte Carlo simulation

ARTICLE *in* THE JOURNAL OF CHEMICAL PHYSICS · SEPTEMBER 2009

Impact Factor: 2.95 · DOI: 10.1063/1.3225140 · Source: OAI

3 AUTHORS, INCLUDING:

Akihiko Matsuyama
Kyushu Institute of Technology
72 PUBLICATIONS **796** CITATIONS

Packaging-ejection phase transitions of a polymer chain: Theory and Monte Carlo simulation

Akihiko Matsuyama,[a] Masato Yano, and Akiyoshi Matsuda
Department of Bioscience and Bioinformatics, Faculty of Computer Science and System Engineering, Kyushu Institute of Technology, Kawazu 680-4, Iizuka, Fukuoka 820-8502, Japan

(Received 4 March 2009; accepted 19 August 2009; published online 11 September 2009)

We theoretically study packaging-ejection phase transitions of a flexible polymer chain, translocating through a spherical cavity. Based on the Flory model for coil-globule transitions of a single flexible polymer, we derive the free energy of the polymer chain through a spherical cavity. Depending on the size of the cavity, the attractive interaction between the polymer and cavity, solvent quality, and the length of the polymer chain, we find continuous and discontinuous phase transitions between a packaged state and an ejected one of the polymer chain. These results suggest a possibility of the control of DNA packing and ejection. We also perform a Monte Carlo simulation to confirm the theoretical results. © *2009 American Institute of Physics*. [doi:10.1063/1.3225140]

I. INTRODUCTION

Translocations of a polymer chain through a pore play an important role for many biological processes and for biotechnological applications. The problems of polymer translocations, including DNA packing and ejection, received recently great attention of experimental and theoretical studies. For instance, proteins are transported through channels in a biological membrane.[1–15] DNA inside bacteriophages is ejected into the cytoplasm of a host cell when infection takes place.[16–21] The packing of a double-stranded DNA within capsid provides genome organization in the life cycle of bacteriophage.[22–24]

Packaging and ejection of viral genome are challenging subjects both for molecular biology and polymer physics. The dimension of capsid is typically tens of nanometers and the length of DNA to be packaged into the capsid is generally three to four orders longer. Then the simple coarse-grained model for DNA packing is to consider a polymer chain confined in a spherical cavity. From a theoretical point of view, these systems can be modeled by taking into account electrostatic interactions,[24,25] cavity size,[26,27] rigidity of a polymer chain,[22,28] length of a polymer chain,[22,27] interactions between a polymer and a cavity, and mixing a polymer chain with solvent molecules.[14] When the size of a cavity is larger than the radius of a polymer chain, DNA (polymer) chain remains a state of confinement inside the cavity. On decreasing the radius of the cavity, the number of the conformations of the polymer can produce an entropy force tending to push the chain out of the cavity.

Recent experiments found that in the case of bacteriophage λ, the ejection can be 50% inhibited by varying the external osmotic pressure.[16] Ali *et al.*[21] presented simulations to investigate the effects of solvent quality on the dynamics of flexible and semiflexible polymers ejecting from spherical viral capsids. They fond that the mean ejection time increases and the ejection time distributions are broadened as the solvent quality decreases.[21] Then we can expect that it is possible to control the DNA packing and ejection by tuning not only a solvent quality but also other physical parameters such as the size of capsid, the length of a polymer chain, and the interaction between a capsid and DNA.

Our aim is to study a possibility of the control of DNA packing and ejection. We theoretically study packing and ejection of a flexible polymer chain through a spherical cavity. Based on the Flory model for coil-globule transitions of a single polymer chain,[29] we derive the free energy of the polymer chain by taking into account the elastic free energy, the attractive interaction between the polymer and cavity, and the free energy of a mixing of a polymer with solvent molecules. Such model has also been applied to study a polymer translocation through a pore.[14] Depending on the radius of a cavity and the interaction between a polymer and a cavity, we find phase transitions between a completely packed state, where the polymer segments are packaged inside the cavity, a partially ejected state, where the polymer segments are distributed both inside and outside the cavity, and a completely ejected one. We perform a Monte Carlo (MC) simulation to confirm the results of the mean field theory and study the kinetics of polymer packing and ejection.

II. FREE ENERGY OF A POLYMER ESCAPING FROM A SPHERICAL CAVITY

Consider a flexible polymer chain packed into, and escaped from, a spherical cavity of the radius D. In a thermal equilibrium state, the polymer segments may be distributed both inside and outside the cavity. Figure 1 shows a state of a polymer escaping from a spherical cavity, which includes nonequilibrium and equilibrium states. To derive the equilibrium conformation of the polymer and the fraction of polymer segments inside the cavity, we consider the thermodynamics of the system based on the Flory–Huggins theory,[29] which was a great success in polymer physics.

[a]Electronic mail: matuyama@bio.kyutech.ac.jp. URL: http://iona.bio.kyutech.ac.jp/~aki/.

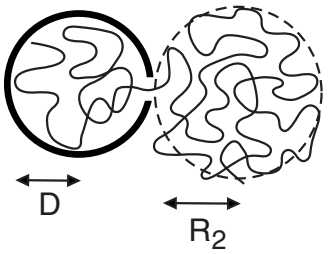

FIG. 1. Schematically illustrated is a snapshot of a polymer chain translocating through a spherical cavity of the radius D. In a thermal equilibrium state, the polymer segments outside the cavity are distributed inside the spherical region of the radius R_2, whose value is determined by minimizing the free energy.

Let n_1 and n_2 be the number of polymer segments inside (side 1) and outside (side 2) the cavity, respectively. We then have $n=n_1+n_2$, where n is the total number of segments on a flexible polymer chain. We here consider that the polymer segments inside the cavity are randomly distributed inside the cavity. Let R_2 be the mean radius of the occupied region of the polymer segments in side 2. We here do not take into account the wall thickness of the cavity. Then the volume fraction of the polymer segments inside the cavity is given by

$$\phi_1 = \tfrac{4}{3}\pi a^3 n_1/\left(\tfrac{4}{3}\pi D^3\right) = a^3 n_1/D^3, \tag{1}$$

and the volume fraction of the segments distributed inside the sphere of the mean radius R_2 is given by

$$\phi_2 = \tfrac{4}{3}\pi a^3 n_2/\left(\tfrac{4}{3}\pi R_2^3\right) = a^3 n_2/R_2^3, \tag{2}$$

where $(4/3)\pi a^3$ corresponds to the volume of a unit segment on the polymer. We here define the expansion factors of the polymer chain due to the deformation in sides 1 and 2 as

$$\alpha_1 = D/R_{0,1}, \tag{3}$$

$$\alpha_2 = R_2/R_{0,2}, \tag{4}$$

respectively, where $R_{0,i}=a\sqrt{n_i}$ is the radius of gyration of the ideal chain with n_i $(i=1,2)$ segments. The radius R_2 of the occupied region of polymer segments outside the cavity depends on solvent qualities such as good, theta, or poor solvent conditions. Then the value of the expansion factor α_2 is determined by minimizing the free energy of the system. Using these expansion factors and n_i, Eqs. (1) and (2) are given by

$$\phi_1 = \frac{n_1}{r^3 n^{3/2}}, \tag{5}$$

$$\phi_2 = \frac{1}{\alpha_2^3\sqrt{n_2}}, \tag{6}$$

where we define the dimensionless radius $r \equiv D/R_0$ and $R_0 = a\sqrt{n}$ is the radius of gyration of the ideal polymer chain. Equation (3) also can be given by

$$\alpha_1 = r\frac{\sqrt{n}}{\sqrt{n_1}}. \tag{7}$$

The equilibrium values of α_2 and n_2 are determined by the free energy of the system. The free energy of the polymer chain is given by

$$F = F_1 + F_2, \tag{8}$$

where F_1 (F_2) shows the free energy of the polymer in side 1 (side 2).

The free energy of the polymer in side 1 is given by

$$F_1 = F_{1,\mathrm{el}} + F_{1,\mathrm{mix}} + F_{\mathrm{int}}, \tag{9}$$

where $F_{1,\mathrm{el}}$ shows the elastic free energy due to the deformation of the polymer segments from the ideal chain. This free energy is given by Flory:[29]

$$\beta F_{1,\mathrm{el}} = \tfrac{3}{2}(\alpha_1^2 - 1) - 3\ln\alpha_1, \tag{10}$$

where $\beta \equiv 1/k_B T$, T is the absolute temperature, and k_B is the Boltzmann constant. The second term in Eq. (9) shows the free energy for a mixing of a polymer chain with solvent molecules inside the cavity and is given by the Flory–Huggins theory,[29]

$$\begin{aligned}\beta F_{1,\mathrm{mix}} &= \frac{D^3}{a^3}[(1-\phi_1)\ln(1-\phi_1) + \chi_1\phi_1(1-\phi_1)], \\ &= \frac{n_1}{\phi_1}[(1-\phi_1)\ln(1-\phi_1) + \chi\phi_1(1-\phi_1)],\end{aligned} \tag{11}$$

where χ shows the Flory–Huggins interaction parameter between a polymer segment and a solvent molecule. We here assume that the translational entropy term $(\phi_1/n)\ln\phi_1$ of the polymer chain can be neglected since the center of gravity of the polymer chain is fixed near a hole of the cavity in a thermal equilibrium state. The prefactor D^3/a^3 is the total number of segments, including polymer segments and solvent molecules, in side 1. The first and second terms in Eq. (9) have been used for coil-globule transitions of a single flexible polymer chain.[29] The free energy F_{int} in Eq. (9) shows the interaction between the polymer and the cavity and we here assume

$$\beta F_{\mathrm{int}} = -\beta\epsilon_0 n_1 = -\epsilon(n - n_2), \tag{12}$$

where $\epsilon \equiv \beta\epsilon_0$ and $-\epsilon_0$ is the attractive interaction energy between the polymer and cavity. The value of $|\epsilon_0|$ corresponds to the energy difference per a polymer segment between inside and outside the cavity and the positive value of ϵ shows the driving force to pack polymer segments into the cavity. In other words, the ϵ appears as a chemical potential difference trying keep the monomers inside the cavity, which corresponds to the energy difference per a monomer between inside and outside the cavity. In this paper, we assume for simplicity that the free energy F_{int} is linearly dependent on the number n_2 of monomers outside the cavity. For more realistic model of F_{int}, we need to consider adsorption between the cavity surface and the polymer.

The free energy F_2 of the polymer segments in side 2 is given by

$$F_2 = F_{2,\mathrm{el}} + F_{2,\mathrm{mix}}, \tag{13}$$

where $F_{2,\mathrm{el}}$ shows the elastic free energy due to the deformation of the polymer segments and is given by[29]

$$\beta F_{2,\mathrm{el}} = \tfrac{3}{2}(\alpha_2^2 - 1) - 3 \ln \alpha_2, \tag{14}$$

and the free energy for a mixing of a polymer chain with solvent molecules in side 2 is given by

$$\beta F_{2,\mathrm{mix}} = \frac{R_2^3}{a^3}[(1-\phi_2)\ln(1-\phi_2) + \chi\phi_2(1-\phi_2)], \tag{15}$$

$$= \frac{n_2}{\phi_2}[(1-\phi_2)\ln(1-\phi_2) + \chi\phi_2(1-\phi_2)],$$

where the prefactor R_2^3/a^3 is the total number of segments inside the sphere of the radius R_2.

In a thermal equilibrium state, the expansion factor α_2 is determined by minimizing the free energy Eq. (8) with respect to α_2:

$$(\partial F/\partial \alpha_2)_{n_2} = 0. \tag{16}$$

This leads to

$$\alpha_2^2 - 1 + n_2\left[\frac{1}{\phi_2}\ln(1-\phi_2) + 1 + \chi\phi_2\right] = 0. \tag{17}$$

The number n_2 of the polymer segments in side 2 is determined by

$$(\partial F/\partial n_2)_{\alpha_2,} = 0, \tag{18}$$

where we used $n_1 = n - n_2$ before the differentiation. We then obtain

$$\frac{3}{2n_1}(\alpha_1^2 - 1) + \ln(1-\phi_1) + 1 - \chi(1-2\phi_1) + \epsilon + \left(\frac{3}{2\phi_2} - 1\right)\ln(1-\phi_2) + \frac{1}{2} + \chi\left(1 - \frac{\phi_2}{2}\right) = 0. \tag{19}$$

The equilibrium values of α_2 and n_2 are determined from two coupled Eqs. (17) and (19). Using Eqs. (5)–(7), the volume fraction ϕ_i and the expansion factor α_1 are given as a function of α_2 and n_2.

Equation (8) cannot describe a completely packaged state ($n_2=0$) and a completely ejected one ($n_2=1$) because the state of $n_2=0$ (or $n_1=0$) is forbidden in Eqs. (6) and (7). The free energy of the completely packaged state is given by

$$F_1^\circ \equiv F_1(n_1 = n), \tag{20}$$

and that of the completely ejected state is given by

$$F_2^\circ \equiv F_2(n_2 = n). \tag{21}$$

Then, whether the solution of the coupled Eqs. (17) and (19) is a thermal equilibrium state or a metastable one, we have to compare three free energies $F(n_2)$ [Eq. (8)], F_1°, and F_2°. The details are discussed in the next section.

III. PHASE TRANSITIONS OF A POLYMER TRANSLOCATION

In this section we show some numerical results for equilibrium properties of a polymer translocation through a spherical cavity. Figure 2 shows the free energy $f(n_2) \equiv \beta F/n$ [Eq. (8)] plotted against the fraction n_2/n of polymer segments outside the cavity with $\chi=0$ (the good solvent condition) and $n=100$. The reduced radius $r(\equiv D/R_0)$ is changed from curve to curve, where $R_0(=a\sqrt{n})$ is the radius of gyration of an ideal polymer chain in a theta solvent condition. The closed circles at $n_2=0$ show the free energy $f_1^\circ(\equiv \beta F_1^\circ/n)$ of the completely packed state and the free energy f_1° depends on the value of r. The closed circle at $n_2=n$ shows the free energy $f_2^\circ(\equiv \beta F_2^\circ/n)$ of the completely ejected state and the free energy f_2° does not depend on the value of r. To derive the thermal equilibrium state, we compare three free energies Eq. (8), f_1°, and f_2°. Figure 2(a) shows the free energies for $\epsilon=0.1$, corresponding to a weak attractive interaction between the cavity and the polymer. When the radius r is large, the free energy f_1° at $n_2=0$ becomes a minimum, where all polymer segments exist inside the cavity, corresponding to a completely packed state. On decreasing the radius r, the free energy $f(n_2)$ has two minimums and one maximum. When $r=0.86$, we have $f_1^\circ = f(n_2/n \simeq 0.31)$, where the first-order phase transition from a completely packed state ($n_2=0$) to a partially packed one ($n_2 \simeq 0.31n$) takes place. On decreasing the radius r, the minimum of the free energy $f(n_2)$ at $n_2/n > 0.31$ becomes lower than the free energy f_1° and we then have a partially packed state, where the polymer segments are distributed both inside and outside the cavity. When $r=0.4$, the minimum of the free energy $f(n_2)$ at $n_2 \simeq 0.9$ becomes equal to the free energy f_2° at $n_2=n$ and we then have another first-order phase transition from a partially packed state ($n_2 \simeq 0.9$) to a completely ejected one ($n_2=n$). When $r<0.4$, the completely ejected state becomes thermodynamically stable.

On increasing the attractive interaction ϵ between the polymer and the cavity, the mechanism of the phase transition changes. Figure 2(b) shows the free energy for $\epsilon=1$, which corresponds to a strong attractive condition. In this case, the attractive interaction F_{int} between the cavity and the polymer becomes dominant in the free energy F. Because the interaction [Eq. (12)] is linearly dependent on the number n_2

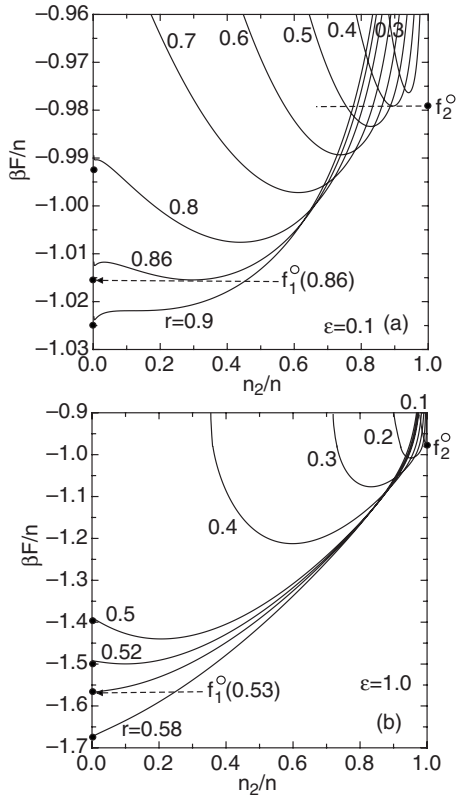

FIG. 2. Free energy [Eq. (8)] plotted against n_2/n for various values of $r(\equiv D/R_0)$ with $\chi=0$, $n=100$, and (a) $\epsilon=0.1$; (b) $\epsilon=1$. See text for details.

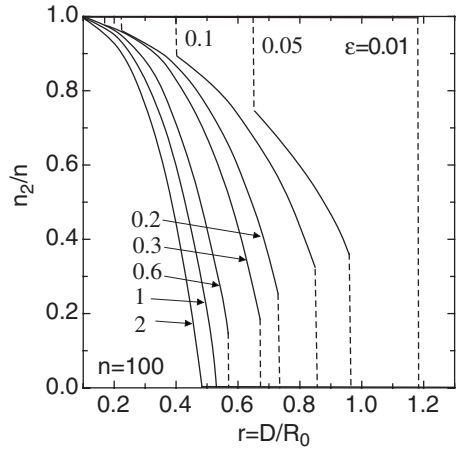

FIG. 3. Fraction n_2/n of the polymer segments outside the cavity as a function of the radius $r(\equiv D/R_0)$ for $n=100$ and $\chi=0$. The interaction parameter ϵ between the polymer and cavity is changed.

with a positive slope, the maximum of the free energy near $n_2 \simeq 0$, shown in Fig. 2(a), disappears and the free energy has only one minimum. When the value of r is large, the free energy f_1° at $n_2=0$ becomes a minimum and a completely packed state is stable. At $r=0.53$, we have the second-order (continuous) packing-ejection phase transition, where a completely packed state is continuously changed to a partially packed one. On decreasing r, the minimum in the free energy $f(n_2)$ becomes lower than the free energy f_1°. When $r=0.1$, the minimum of the free energy $f(n_2)$ becomes equal to the free energy f_2° at $n_2=n$ and we have another continuous phase transition from a partially packed state to a completely ejected one ($n_2=n$). As shown in Fig. 2, the nature of the phase transition can be changed, depending on the strength of the attractive interaction.

This is similar with the Landau–de Gennes theory of a nematic-isotropic phase transition in liquid crystals:[30] The first-order nematic-isotropic phase transition changes to the second-order one when an external field, such as electric or magnetic field, is applied to the system, where the free energy due to the external field is proportional to a nematic order parameter. In our system, the external field corresponds to the attractive interaction between the cavity and the polymer and is assumed to be linearly dependent on the number n_1 in Eq. (12). The value of n_1 corresponds to a scalar order parameter in our model. Then we can expect that the packing-ejection phase transition becomes the second-order one when the interaction is strong.

Figure 3 shows the fraction n_2/n of the polymer segments outside the cavity plotted as a function of the radius $r(\equiv D/R_0)$ for $n=100$ and $\chi=0$. The interaction parameter ϵ between the polymer segment and cavity is changed. The solid curves correspond to the equilibrium value of n_2 and the dashed lines show the first-order phase transition. When the interaction between the polymer and the cavity is weak ($\epsilon=0.01$), we have the first-order packing-ejection phase transition from $n_2=0$ to $n_2=n$ at $r \simeq 1.19$. On decreasing the radius of the cavity, the number of the conformations of the polymer can produce an entropy force tending to push the chain out of the cavity. This is the mechanism of the packing-ejection phase transitions. For smaller values of $r(<1.19)$, all polymer segments exist outside the cavity ($n_2=n$). When $\epsilon=0$, we have no phase transition and all polymer segments exists outside the cavity because the free energy f_2° becomes always minimum, although we have metastable solutions of the free energy Eq. (8). As shown in Fig. 2(a), the phase transition for $\epsilon=0.1$ takes place at $r=0.86$ and $r=0.4$. For values of $0.4<r<0.86$, we have a partially packed state of the polymer chain. On increasing the attractive interaction ϵ, the phase transition point shifts to the smaller values of r and we have the continuous packing-ejection phase transitions as discussed in Fig. 2(b).

Figure 4 shows the expansion factors α_1 [Fig. 4(a)] and α_2 [Fig. 4(b)] as a function of the radius D/R_0 for $n=100$ and $\chi=0$. The interaction parameter ϵ between the polymer segment and cavity is changed. For values of large r, most polymer segments exist inside the cavity (side 1) and the value of the expansion factor α_1 almost does not depend on the ϵ. On decreasing r, the value of n_2 discontinuously increases at the transition point.

Figure 5 shows the phase diagram curve on the $r-\epsilon$ plane for $n=100$ and $\chi=0$. The solid curve corresponds to the discontinuous packing-ejection phase transition and the dashed-curve shows the continuous one. For large values of r and ϵ, the polymer chain is in the completely packed state, where all polymer segments exist inside the cavity. On decreasing the radius r, we have the partially packed state, where polymer segments are distributed both inside and outside the cavity. Further decreasing r, the polymer chain becomes the completely ejected state, where all polymer seg-

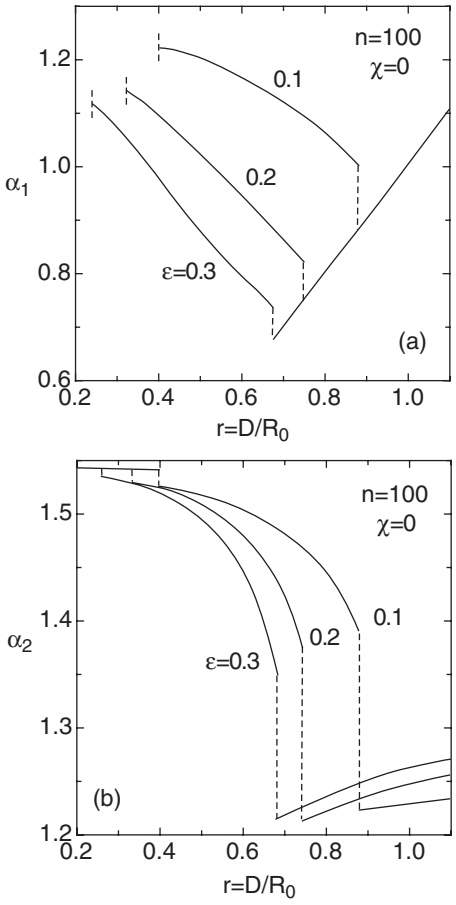

FIG. 4. Expansion factors (a) α_1 and (b) α_2 as a function of the radius $r(=D/R_0)$ for $n=100$ and $\chi=0$. The interaction parameter ϵ between the polymer and cavity is changed.

ments exist outside the cavity. We find that the packing-ejection transition depends on the radius r and ϵ. The closed circle shows the tricritical point, where the first-order phase transition (solid curve) meets the second-order one (dashed curve). We also find a triple point where three phase transition curves intersect. When the value of ϵ is small, we have direct packing-ejection phase transitions without partially

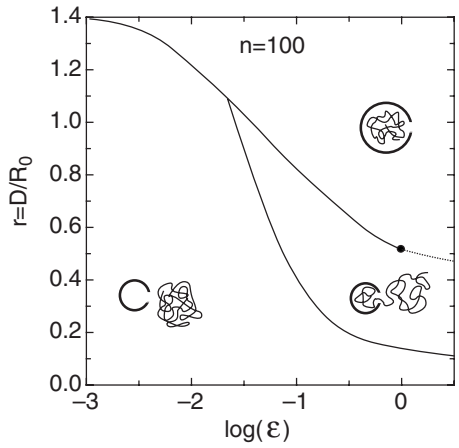

FIG. 5. Phase transition curve on the r (radius)-ϵ (attractive interaction) plane for $n=100$ and $\chi=0$. We find the packing-ejection phase transition depending on the radius r and ϵ. The closed circle shows the tricritical point, where the first-order phase transition (solid curve) meets the second-order one (dashed curve).

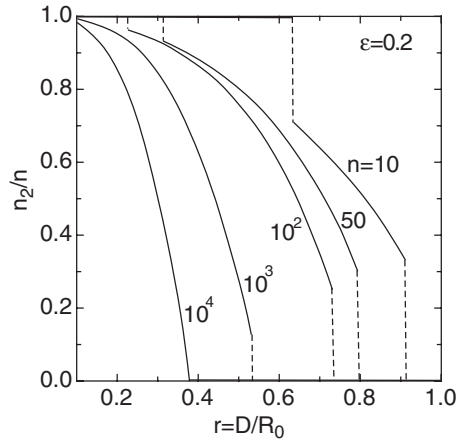

FIG. 6. Fraction n_2/n of the polymer segments outside the cavity as a function of the reduced radius $r(\equiv D/R_0)$ for $\epsilon=0.2$ and $\chi=0$. The number n of the polymer segments is changed.

packed states. (Note that, for $\epsilon=0$, the completely ejected state is always stable). When all segments are packed into the cavity, the volume fraction of polymer segments inside the cavity is given by $\phi_1=1/(r^3\sqrt{n})$ from Eq. (5). For a typical bacteriophage, we have $\phi_1\simeq 0.4$, which corresponds to $r\simeq 0.63$. Then, for a polymer of $n=100$, we need at least $\epsilon > 0.45$ to pack the flexible polymer into the cavity.

Figure 6 shows the fraction n_2/n of the polymer segments outside the cavity as a function of the reduced radius r for $\epsilon=0.2$ and $\chi=0$. The number n of polymer segments is changed from curve to curve. For small values of n, we have the first-order packing-ejection phase transitions with decreasing the radius r. On increasing n, the packing-ejection phase transition occurs at smaller values of the reduced radius (r) and the packing-ejection phase transition is changed from a discontinuous to a continuous one. (Note that the horizontal axis is normalized by $R_0=a\sqrt{n}$ and then the phase transition takes place at larger values of D with increasing n.) We see that, from Eq. (12), for larger values of n, the attractive interaction F_{int} becomes dominant in the free energy. Then the first order-packing-ejection phase transition becomes the second-order one with increasing n as discussed in Fig. 2.

The effects of solvent quality can also change the nature of the phase transition. When the solvent condition χ is changed, the curves of n_2/n in Fig. 3 are affected. On increasing χ, or poorer solvents, the phase transition point shifts to smaller values of D/R_0 and the phase transition is changed from a discontinuous to a continuous one, although it is not shown in this paper. The value of n_2 decreases with increasing χ. For example, when $\epsilon=0.2$, $n=100$, and $\chi=0.6$, the value of n_2 continuously increases with D/R_0 from $D/R_0\simeq 0.55$. This means that the driving force for the polymer ejection decreases as the solvent becomes poorer. This result qualitatively agrees with the results of a recent experiment[16] and a simulation.[21]

IV. MONTE CARLO SIMULATIONS

In this section we perform the MC simulation to confirm the mean field theory, discussed in the previous section. We also briefly discuss the kinetics of the polymer translocation through a spherical cavity.

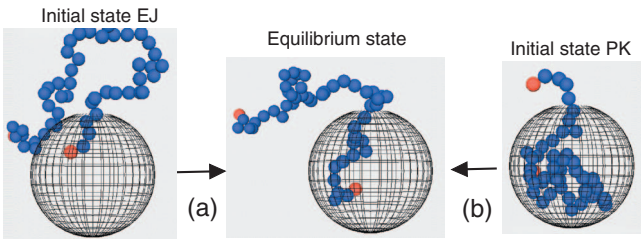

FIG. 7. Snapshot of a polymer translocating through a pore on a spherical cavity: packing (a) and ejecting (b) processes.

Consider a spherical cavity of radius D and the wall thickness d. The cavity has a pore of radius h and a polymer chain can go through this pore. A pearl-necklace chain of n beads consists of $n-1$ freely jointed rigid bonds of length a. Any bead obeys the self-avoiding walk statistics to realize the good solvent condition ($\chi=0$), which is discussed in the previous section. The potential of polymer segments inside the cavity is given by $U=-\epsilon n_1$ as treated in Eq. (12). The interaction between the surface of the cavity and the polymer is taken as a hard wall. The dynamics of the polymer translocation through the cavity can be simulated by a dynamic MC method. In the present method, an elementary attempted MC move is performed by picking an effective (ith) bead at random and trying to displace it from its old position to a new one with kink-jump dynamics.[31,32] After the ith bead has been chosen at random, the bead is moved without collision with the other beads from its old position $\mathbf{r}_i$ to a new one $\mathbf{r}_i'$, located a randomly chosen angle ψ, keeping the neighboring beads $\mathbf{r}_{i-1}$ and $\mathbf{r}_{i+1}$ fixed. If the ith bead at $\mathbf{r}_i'$ is penetrating another bead of the chain, this attempt is rejected and the ith bead remains at $\mathbf{r}_i$, otherwise the new position $\mathbf{r}_i'$ is accepted as a new configuration if these trial moves pass the standard Metropolis acceptance test,[32] using the potential U. In this manner, a sequence of new configurations is generated. As shown in Fig. 7, in our simulation model, we set that both end segments (red circles) of the polymer always exist inside and outside the cavity because the mean field theory [Eq. (8)] holds for $0<n_i<n$. We here take $a=0.5$, $d=0.6$, $h=0.7$, and $n=50$ for a typical example

For the initial state of our simulations, we examine two types of the initial conditions. One is that a few monomer of the chain is inside the cavity, while all the other beads are outside the cavity. We refer this as "ejecting (EJ) state." The other is that a few monomer of the chain is outside the cavity, while the other beads are inside the cavity. We refer this as "packaging (PK) state." With time, the polymer chain moves to a thermal equilibrium state from the initial state. Figure 7 shows the packing (a) and ejecting (b) processes in our simulations. The simulation data presented in this paper reflect a statistical average over $M=2000$ repetitions with 10^7 MC steps. We confirmed that, in a bulk solution, the gyration radius of the polymer chain is given by $R_G=an^{\nu}$, where $\nu\simeq 0.6$ corresponding to a good solvent condition.

A. Packing-ejection phase transition

In this subsection, we consider the equilibrium properties of the polymer translocation through the cavity. Figure 8 shows the comparison of the theoretical calculation (solid lines) with the MC simulation (symbols) for $n=50$. The equilibrium values of the number n_2 of segments outside the cavity for $\epsilon=0$ (triangles), $\epsilon=0.2$ (open circles), and $\epsilon=0.3$ (solid circles) are plotted against the reduced radius D/R_G, where the radius D is normalized by the gyration radius $R_G(\equiv an^{3/5})$ of the polymer chain in the good solvent condition: $\chi=0$. Using r we have $D/R_G=n^{-0.1}r$. The solid curves for $\epsilon=0.2$ and $\epsilon=0.3$ show the equilibrium values, calculated by the three free energies: F, F_1°, and F_2°. The solid curve for $\epsilon=0$ is the metastable state, calculated by the free energy F, or the coupled equation: Eqs. (17) and (19). When $\epsilon=0$, the completely ejected state is thermodynamically stable as discussed in the previous section. In our MC simulations, we set at least one end segment exists inside the cavity, then we have the partially ejected state even if $\epsilon=0$. For large values of D, most polymer segments exist inside the cavity. On decreasing the radius D, the polymer segments inside the cavity are ejected by the entropic force of polymer segments inside the cavity. On increasing ϵ, the value of n_2 decreases. We confirm that the results of the mean field theory are qualitatively consistent with that of the MC simulations.

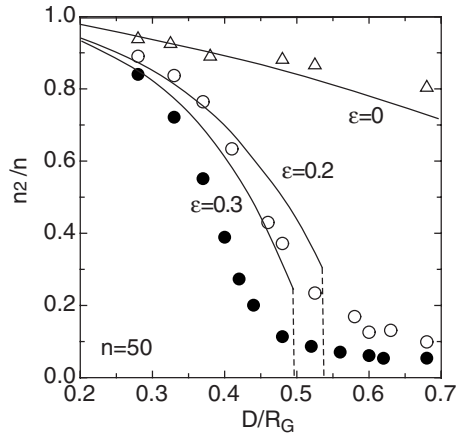

FIG. 8. Comparison of the mean field theory (curves) with the MC simulation (symbols). The equilibrium values of n_2 are plotted against the reduced radius D/R_G, where $R_G(\equiv an^{3/5})$.

B. Translocation time to an equilibrium state

In this subsection we study translocation time for packing and ejecting processes. In our simulations, we used two types of initial conditions: PK and EJ states. We here show the differences of the time evolution of these two cases.

Figure 9 shows the time evolution of n_1 plotted against MC steps for $D/R_G=0.38$ with $\epsilon=0$. The solid circles show the time evolution of the initial state PK (ejecting process) and the open circles show the time evolution of the initial state EJ (packing process). With time, the value of n_1 reaches its equilibrium value (plateau region). However there is the difference in the translocation time to reach its equilibrium value. In the case of the initial state PK, where most polymer segments initially exist inside the cavity, polymer segments move to outside the cavity and the value of n_1 decreases toward its equilibrium value with time. On the other hand, in the case of the initial state EJ, where most polymer segments

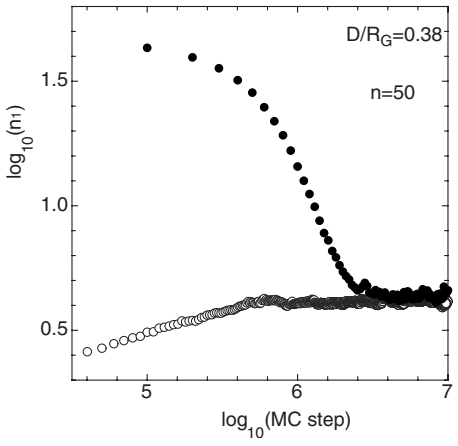

FIG. 9. Time evolution of number n_1 of the polymer segments inside the cavity plotted against MC steps for $D/R_G=0.38$ with $\epsilon=0$. The solid circles show the time evolution of the initial state PK and the open circles show the time evolution of the initial state EJ.

initially exist outside the cavity, polymer segments move to inside the cavity and the value of n_1 increases toward its equilibrium value. The packing time τ_p can be defined as the time to reach the equilibrium value of n_1 from the initial state EJ. On the other hand, the ejection time τ_e can be defined as the time to reach the equilibrium value of n_1 from the initial state PK. Figure 9 shows that the packing time τ_p is faster than the ejection time τ_e.

Figure 10 shows the ejection time τ_e (solid circles) and the packing time τ_p (open circles) plotted against the radius D/R_G with $n=50$ and $\epsilon=0$ (note the log-log plot). We find that $\tau_e > \tau_p$ in our simulation region, namely, it takes longer time to eject polymer segments to outside the cavity rather than packing of polymer segments, because the equilibrium value of n_1 is small and most segments are outside the cavity in an equilibrium state. In the case of the packing process, most polymer segments already exist outside the cavity at the initial stage of a translocation run and few polymer segments move to inside the cavity with time. Then the packing time τ_p is faster than τ_e. Recent simulations have shown that the packing time is faster than ejection time in the case of a flexible polymer chain with a spherical capsid.[28] The packing

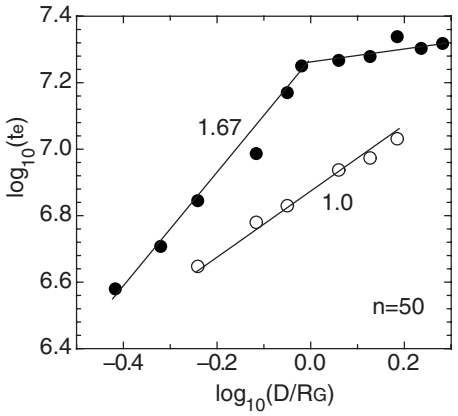

FIG. 10. Ejection time (solid circles) and packing time (open circles) plotted against the radius D/R_G with $n=50$ and $\epsilon=0$. Solid lines are shown as a guide. The slopes are indicated on the figure.

time τ_p increases with increasing D/R_G and there is a region where the packing time τ_p is proportional to D/R_G.

In the case of the ejection process, the escape time τ_e increases with increasing the radius D and becomes almost constant above $D/R_G > 1$. We find the scaling law $\tau_e \propto D^{1.67}$ for $D/R_G < 1$. Due to the well known scaling results,[33] the free energy per chain of confinement inside a sphere of radius D is $F \sim k_B TN/D^{1/\nu}$, where ν is the exponent defined by the n dependence of the gyration radius of the chain in the absence of confinement. Since the free energy per monomer represents the chemical potential difference that drives the translocation, $\Delta\mu = F/N$, the escape time can be estimated as $\tau_e \sim N/\Delta\mu \sim ND^m$,[7,26] where $m \equiv 1/\nu$. For self-avoiding polymers ($\nu=3/5$), we get $m=1.666$. The result of our simulation is consistent with the prediction of the scaling theory. Recent simulation study shows stronger dependence on the radius of the cavity.[26] In our simulations the volume fraction of polymer in the cavity is small and then our results correspond to a weak confinement regime.[34] When the radius of the cavity is larger than the gyration radius of a polymer chain, $D/R_G > 1$, elastic penalty due to the confinement of the polymer chain becomes small and the ejection time becomes almost constant. The effect of the attractive interaction between polymer and cavity can drastically change the translocation processes.[35]

V. SUMMARY

We studied the packing and ejection of a flexible polymer translocating through a spherical cavity. Based on the Flory model for coil-globule transitions of a single polymer chain, we derive the free energy of the polymer chain by taking into account the elastic free energy, the free energy of a mixing of a polymer and solvent molecules, and the attractive interaction between the cavity and the polymer. We predict the discontinuous and continuous packing-ejection phase transitions, depending on the cavity size, the polymer-cavity interaction, solvent quality, and the length of the polymer chain. These results suggest a possibility on the control of DNA packing and ejection. We also perform a MC simulation to confirm the mean field theory and study the kinetics of polymer translocations through a spherical cavity. The results of the mean field theory are qualitatively in agreement with that of the MC simulations.

In this paper we focus on the packing and ejection of a flexible polymer. The semiflexibility of a polymer chain and the adsorption of polymer segments onto the cavity surface are also important to the packing and ejection of double-strand DNAs. We will further study polymer packing and ejection by taking into account these effects.

ACKNOWLEDGMENTS

This work was supported by Grant-in Aid for Scientific Research (C) and that on Priority Area "Soft Matter Physics" from the Ministry of Education, Culture, Sports, Science and Technology of Japan.

[1] J. J. Kasianowicz, E. Brandin, D. Branton, and D. Deamer, Proc. Natl. Acad. Sci. U.S.A. **93**, 13770 (1996).
[2] A. Meller, L. Nivon, and D. Branton, Phys. Rev. Lett. **86**, 3435 (2001).
[3] S. E. Henrickson, M. Misakian, B. Robertson, and J. J. Kasianowicz, Phys. Rev. Lett. **85**, 3057 (2000).
[4] A. Baumgartner and J. Skolnick, Phys. Rev. Lett. **74**, 2142 (1995).
[5] W. Sung and P. J. Park, Phys. Rev. Lett. **77**, 783 (1996).
[6] M. Muthukumar, J. Chem. Phys. **111**, 10371 (1999).
[7] M. Muthukumar, Phys. Rev. Lett. **86**, 3188 (2001).
[8] D. K. Lubensky and D. R. Nelson, Biophys. J. **77**, 1824 (1999).
[9] S. Chern, A. E. Cardenas, and R. D. Coalson, J. Chem. Phys. **115**, 7772 (2001).
[10] T. Ambjornsson, S. P. Apell, Z. Konkoli, E. A. Di Marzio, and J. J. Kasianowicz, J. Chem. Phys. **117**, 4063 (2002).
[11] P. Tian and G. D. Smith, J. Chem. Phys. **119**, 11475 (2003).
[12] E. Slonkina and A. B. Kolomeisky, J. Chem. Phys. **118**, 7112 (2003).
[13] E. A. Di Marzio and J. J. Kasianowicz, J. Chem. Phys. **119**, 6378 (2003).
[14] A. Matsuyama, J. Chem. Phys. **121**, 604 (2004); **121**, 8098 (2004).
[15] S. Tsuchiya and A. Matsuyama, Phys. Rev. E **76**, 011801 (2007).
[16] A. Evilevitch, L. Lavelle, C. M. Knobler, E. Raspaud, and W. M. Gelbart, Proc. Natl. Acad. Sci. U.S.A. **100**, 9292 (2003).
[17] M. de Frutos, S. Brasiles, P. Tavares, and E. Raspaud, Eur. Phys. J. E **17**, 429 (2005).
[18] D. Lof, K. Schillen, B. Jonsson, and A. Evilevitch, J. Mol. Biol. **368**, 55 (2007).
[19] M. Castelnovo and A. Evilevitch, Eur. Phys. J. E **24**, 9 (2007).
[20] C. Sao-Jose, M. de Frutos, E. Raspaud, M. A. Santos, and P. Tavares, J. Mol. Biol. **374**, 346 (2007).
[21] I. Ali, D. Marenduzzo, and J. M. Yaomans, Biophys. J. **94**, 4159 (2008).
[22] C. Forrey and M. Muthukumar, Biophys. J. **91**, 25 (2006).
[23] A. Cuervo, M. C. Vaney, A. A. Antson, P. Tavares, and L. Oliveira, J. Biol. Chem. **282**, 18907 (2007).
[24] D. Marenduzzo, Comp. Math., Meth. in Medi. **9**, 317 (2008).
[25] Z. Li, J. Wu, and Z. G. Wang, Biophys. J. **107**, 112508 (2007).
[26] A. Cacciuto and E. Luijten, Phys. Rev. Lett. **96**, 238104 (2006).
[27] A. Cacciuto and E. Luijten, Nano Lett. **6**, 901 (2006).
[28] I. Ali, D. Marenduzzo, and J. M. Yaomans, Phys. Rev. Lett. **96**, 208102 (2006).
[29] P. J. Flory, *Principles of Polymer Chemistry* (Cornell University, Ithaca, 1953).
[30] P. G. de Gennes and J. Prost, *The Physics of Liquid Crystals*, 2nd ed. (Oxford Science, London, 1993).
[31] M. Muthukumar and A. Baumgartner, Macromolecules **22**, 1937 (1989).
[32] *Monte Carlo and Molecular Dynamic Simulations in Polymer Science*, edited by K. Binder (Oxford University Press, New York, 1995).
[33] P. G. de Gennes, *Scaling Concepts of Polymer Physics* (Cornell University Press, Ithaca, NY, 1979).
[34] T. Sakaue and E. Raphael, Macromolecules **39**, 2621 (2006).
[35] Due to our preliminary simulations, the value of the exponent m for the ejection time (τ_e) increases with increasing the attractive interaction ϵ.